DSS 14 X-Band Radar Feedcone

D. E. Neff and D. A. Bathker
Communications Elements Research Section

A high-power 400-kW continuous-wave (CW) X-band radar feed system is described for use with the Goldstone, California, 64-m DSS 14 antenna system. Design considerations, their solutions, and final system testing are discussed. The radar system, unique in terms of antenna size, radiated power, and efficiency, became operational in December 1974.

I. Introduction

There were two aspects to the feed development for the DSS 14 400-kW X-band radar: the radar feed system and hardware design and the integration of all elements within a new antenna feedcone. At the start of this project, an existing research feedcone then in use at DSS 14 (MXK for multiple X-band, K-band) contained wide-band X-band and separate K-band receiving systems. Both front end systems performed with high feed efficiency and very low noise levels (Refs. 1, 2, 3, and 4).

II. Radar Feed System Design

A new feedcone was planned, based on retention of all existing research capabilities, the addition of a high-power radar feed, and integration of the transmitter within. The new feedcone (XKR for X-band, K-band, radar) would occupy the 64-m-diameter antenna Bay 1 research and development position on the DSS 14 tricone. As shown in Figs. 1 and 2, the tricone structure consists of three bays, or feedcone locations. The upper two feedcone locations are reserved for the network operational S/X-band radio system. Each of the upper feed cone locations includes one subreflector stop or focal position, providing perfect overall antenna system (axial) pointing. The lower feedcone location includes three subreflector stops, 1R, 1, and 1L, each providing perfect antenna system pointing when the subreflector is so positioned. Of course, only one focal position may be used at a given time (with the exception of the operational position of the S/X-band reflex dichroic feed system on the upper two feedcones, Fig. 2). Each of the three available research focal positions is occupied in the new feedcone design, as shown in Fig. 1.

The major consideration in the X-band radar feed system design was the polarization selection technique. Right-hand or left-hand circular polarization (RCP or LCP) was required for transmission, with the opposite polarization required for "matched" reception (accounting for signal phase reversal after reflection) and the same polarization desired (but not mandatory) for "crossed" reception experiments. Several common waveguide

devices (turnstile junction, orthomode transducer, quarter-wave plate between rotary joints) have provided switchable polarization in high-CW-power planetary radars. In the case of the X-band 400-kW radar, it was necessary to commit to acceptable performance by a firmly established date: the Saturn ring opportunity of January 1975. The high risk of waveguide breakdown failures in the candidate waveguide devices indicated that a more reliable polarization selection technique was needed.

The plan evolved was as follows: One of the waveguide devices would be selected for further development, with a goal of providing an operationally simple yet reliable conventional switched feed polarizing system. In parallel, a nonswitched (fixed polarization) feed would be developed for the high-power transmit function. The tricone subreflector focus position would be the switch element, alternating between transmit and receive feedhorns (1L to 1 in Fig. 1) during the transmit/receive changeovers. Even though questions of 64-m antenna system quadripod dynamic behavior (damping time) and subreflector motor/gearing wearout arose, this proposed mode remained the primary backup to assure a functional X-band radar by January 1975.

Once the above system planning, with backup provision, was established, the X-band portion of the complete XKR feedcone block diagram was completed (Fig. 3). The preferred radar operation would be as follows: transmission and reception would both occur through the radar feed, with the subreflector fix-focused in the 1L position; switching from radar-transmit to radar-receive would be accomplished by rotating the high-power polarization switch and changing the transmit/receive switch. The wideband receive feed would serve as the backup receive system for the radar as well as continue in use for the normal radio science and DSN development activities.

III. Radar Feed Component Design

As mentioned above, the major system and component consideration for the radar feed was the polarization selection technique. Use of a waveguide orthomode coupler, together with a fixed circular polarizing device, was considered, but no acceptable low-power design was available for modification to serve at high power. Further, breakdown risk exists due to complex fields within orthomode couplers. Rotary joints, in TE_{11} mode cylindrical waveguide, have given reliable 400-kW service in DSN operational and planetary radar systems at S-band (with obvious larger-size waveguide and attendant lower internal field strengths). At X-band, the scaled diameter of the rotary joint cylindrical waveguide, 34.77 mm (1.369 in.), provides a theoretical breakdown level (based on 30×10^5 V/m) of 4.4 megawatts (MW). The 34.77-mm cylindrical waveguide (WC137), compared with the other system waveguide (WR125), which has a theoretical breakdown level of 2.5 MW, appears acceptable. This is further enhanced when derating factors are introduced (Ref. 5). For WR125, practical considerations lead to a derating factor of 0.28, or 0.70 MW maximum rating. For WC137, the derating factor is estimated at 0.40, or 1.8 MW maximum rating. Thus, the cylindrical WC137 waveguide is stressed a factor of 2.5 less (in power) than the rectangular WR125 waveguide.

Despite relatively unknown electric field conditions present within the choke assemblies of such TE_{11} mode rotary joints, the risk vs. payoff of adopting this approach for further development appeared acceptable. Similar choke assemblies used in rectangular waveguide switches had previously given good service at 100 kW CW in WR112 at 7150 MHz, an earlier JPL lunar radar. It is interesting to note that in this previous experience, 100-kW operations were conducted within a waveguide having a derated maximum power ability of 400 kW, or a 4:1 power safety margin. In the new radar, the WR125 rectangular waveguide provides only a 1.75:1 power safety margin (0.70/0.40). The WC137 provides a 4.5:1 power margin (1.8/0.40). Clearly, careful attention to details such as waveguide internal cleanliness, surface finish, and avoidance of hot spots was recognized necessary for successful operation of the new radar with such a slim safety margin, particularly in the WR125 rectangular waveguide portion.

The radar feed assembly consists of three major parts; the hybrid mode (TE- and TM-component) corrugated waveguide horn, the quarterwave plate polarizer, and the transition from cylindrical to rectangular waveguide. The parts are constructed principally of OFHC copper, with reduced microwave path lengths and nonflanged waveguide joints where possible to minimize dissipation loss and resultant heating. One primary difference between the radar feed assembly and the older existing low-power wideband receive feed assembly is in a feedhorn matching device. As will be described in the performance section, the low-power receive feedhorn is matched in such a way (with a dual iris section) as to provide good polarization axial ratio (or ellipticity) at two frequencies: the DSN receive band at 8.4 GHz and the cooperative Goldstack radar (and radio science very long baseline interferometry (VLBI)) frequency near 7.8 GHz. For the high-power radar, the matching device was too risky from a breakdown viewpoint; it was eliminated in the high-power design.

Figure 4 presents a cross section of the radar feed assembly, showing the three major parts:

(1) Hybrid mode feedhorn. The low-power design of the corrugated waveguide horn has been discussed elsewhere (Ref. 6). The high-power horn assembly utilizes the internal structure of the low-power design, differing only in the added water cooling and round waveguide connections. The high-power horn is divided into four sections, each approximately 150 mm long. The feedcone roof is used to provide a heat sink for the larger-diameter (lower dissipation loss) aluminum sections (see Fig. 8) at the connection between the aperture and third sections. The smaller-diameter (higher dissipation loss) first and second sections are made of OFHC copper, with water cooling jackets. Three flanges are used in the larger sections of the horn; bolts are placed on approximately 15-mm centers. The small-diameter end of the horn is an integral part of one rotary joint, as shown in Fig. 4.

(2) Polarizer section. The polarizer section converts a linearly polarized TE°_{11} mode into a circularly polarized (RCP or LCP) TE°_{11} mode through quarterwave plate action. No flanges are used in this section; the breakpoints are designed as integral parts of the rotary joints, as shown in Fig. 4. OFHC copper construction is used with water cooling jackets. In this section, water cooling not only inhibits elevated surface (and possible particulate debris) temperatures; it also limits thermal expansion of the critical rotary joint bearings and choke details. The theoretical loss of cylindrical copper WC137 waveguide used in the polarizer section is approximately 0.040 dB/m (0.012 dB/ft); 4.6 kW/m (1.4 kW/ft) is dissipated. Thermal expansion is worrisome since clearances between rotating surfaces are only 0.125 to 0.250 mm (0.005 to 0.010 in.). Pressurization gas seals are used to minimize leakage of the 0.22 N/cm^2 (5-oz/$in.^2$) nitrogen used in the waveguide system. As mentioned, relatively unknown electric field conditions in the choke details remains a minor risk with this section.

(3) Waveguide transition. A smooth, tapered transition from cylindrical WC137 to rectangular WR125 waveguide was available from a previous program. With the exception of water jacket and integral rotary joint details, no design was required. While this transition is relatively long, as seen in Fig. 4 (with resultant dissipation loss), use of a shorter four-section stepped transition (as in the wideband receive feed assembly) was discarded on the basis of complex field conditions within, particularly in this case of an unfiltered transmitter output, with possible resultant harmonic fields in the output transmission lines.

IV. Radar Feed Component Testing

Early development tests consisting of feedhorn pattern and polarizer ellipticity (July 1973–March 1974) were conducted using the 20-m anechoic chamber at the JPL Mesa Antenna Range. Medium-power tests (March 1974–September 1974) were conducted at the DSS 13 transmitter building. High-power testing was started at DSS 14 (November 1974) on the antenna and continues as time permits.

A. Antenna Range Tests

The antenna range tests consisted of selecting the proper cylindrical waveguide phasing sections and exact quarterwave plate length for the 8495-MHz radar frequency. The development phase was extended due to the fact that an OFHC copper materials shortage developed and fabrication was delayed. Also, the final polarizer and transition sections required fabrication using the electric discharge machine process and required additional time. Final assembly and testing was done in a relatively short period during March 1974.

The radar feed system ellipticity is shown in Fig. 5. The voltage standing wave ratio (VSWR) at 8495 MHz is less than 1.05. Performance below 8450 MHz is a natural function of the quarterwave plate; from 8450 to 8550 MHz, phasing of minor internal mismatches produced a very-high-quality polarization performance.

The low-power wideband receive feed for the XKR feed cone was further developed at this time. Again, cylindrical waveguide phasing sections and exact quarterwave plate length, and (as mentioned) a feedhorn matching device were the development parameters. The feedhorn matching device is a suitably spaced iris pair, weakly resonant (and well matched) at the 8.4-GHz band; simultaneously, the iris pair provides a desired reflection coefficient (magnitude and phase) at the 7.8-GHz band. As seen in Fig. 5, the natural behavior of 8.4-GHz design quarterwave plate of the type used here is to provide approximately 3 dB of ellipticity at 7.8 GHz. This level of cross polarization is considered unacceptable; use of the matching device reflects a specified portion of an outgoing (test) wave. Due to two passes of the reflected wave through the quarterwave plate (and cross-polarized reflection at the input end), the reflected wave exits the

feed primarily at the feedhorn aperture end rather than at the input end. By proper overall phasing, the total outgoing wave can then be corrected in ellipticity, since it then consists of three components: Component A, the desired polarization; Component B, the undesired polarization (these components are output on the first "pass"); and finally, Component C, the twice reflected specified portion, phased to largely cancel Component B. That this technique works is seen in Fig. 6. High-quality polarization performance is obtained in both the 7.8- and 8.4-GHz bands for the wideband receive feed, as is needed for the multi-purpose functions provided by this equipment.

B. DSS 13 Medium-Power Testing

The first medium-power testing was done in a special modified klystron test fixture, mounted on one of the feedcone elevators at the DSS 13 transmitter building. The feedhorn and transmitter were raised as an assembly to allow transmission through a small hole in the roof of the building (Fig. 7). Over a 2–3 month period, both the fixed (backup) and rotary joint feed assemblies were tested. A final test at 170 kW (May 1974) with a single klystron was made on the rotary joint feed for 2-1/2 h. The successful sustained test at 170 kW represented 65% of the expected field strength at 400 kW; with this encouragement, a firm decision was made to install the rotary feed in the new feedcone, in anticipation of full-power dual-klystron tests. Feedcone testing at DSS 13 was later limited to 250 kW due to various problems.

The full assembly of the radar feed unit is shown in Fig. 8. The feedcone roof interface provides a nonrotatable reference; the rectangular waveguide end provides the second reference. The polarization switch drive acts to rotate the quarterwave plate between two stable (and highly repeatable) positions 90 mechanical degrees apart, for LCP or RCP transmission or reception. A closeup of the polarization switch drive is seen in Fig. 9. This rugged mechanism has a built-in dwell feature to permit ring, worm, and motor overtravel during motor coast-down. The cycle time of the mechanism is 6 s; this relatively long switch cycle was considered adequate for the intended initial purpose of the radar.

Figure 10 shows the non-water-jacketed low-power wideband receive feed, ready for feedcone installation. Finally, Fig. 11 shows the top of the completed XKR feedcone. The two X-band horns are seen, as well as the K-band (14–17 GHz) horn. Three future feedhorn mounting locations are visible. Space for a K-band off-axis (reference) horn, as well as the two intermediate locations, is provided. Internal space is, however, another matter. The XKR feedcone, as completed with the dual-klystron 400-kW transmitter in the lower section and three feeds and two traveling wave masers (TWMs) for X- and K-band in the upper section, is very crowded.

C. DSS 14 Antenna High-Power Tests

Early in the initial high-power tests (November 21, 1974), a Kapton 0.075-mm (0.003-in.) horn window was destroyed when a large hole was burned in the surface. Replacement of the horn window with a thinner 0.025-mm (0.001-in.) sheet and cleaning of the connecting waveguide corrected the problem.

The X-band radar feed and feed cone system became operational in December 1974 for the planned Saturn ring experiment and successfully continued transmitting at power levels up to 400 kW into February 1975. No high-power failures of any consequence occurred with the feed during this period.

V. Radar Feedcone RF Performance

After installation at DSS 14, the XKR feedcone was checked at X-band (November 9, 1974) for overall system efficiency (η) and operating system noise temperature (T_{op}), as functions of elevation angle. Both possible receive paths, as shown in the block diagram (Fig. 3), were checked (subreflector 1 and 1L positions in Fig. 1). As expected, overall antenna system pointing was the same on either receive path, verifying the excellent subreflector positioning (and feedhorn placement accuracy within the feedcone) previously observed with the DSS 14 antenna mechanical system.

Figures 12 and 13 show the measured performance. As is normal for DSN 64-m antenna systems operated at X-band, subreflector z-axis focussing, as a function of elevation angle, is necessary, and the effects of proper focussing are included in the data. The term "receiving conditions only" in Fig. 11 refers to the fact that the measurements are done with a radio star. It is possible (although unlikely) that some performance degradation might occur under transmitting conditions. In Fig. 12, overall system efficiency includes effects of the normally clear Earth atmosphere (as is usually encountered in operations). Also, it should be noted in Fig. 12 that the two efficiencies given are both for receiving conditions referenced to the TWM input. (More on transmitting conditions later.) Overall efficiencies of 46 and 45% are indicated for the two receive systems, or approximately 0.10 dB difference. This unexpectedly high difference was thought, at the time, to arise in either the transmit/receive switch or WR125/WR112 waveguide intercon-

necting piece (Fig. 3). Figure 13, which shows the operating noise level, basically confirms the radio star data; at zenith, the radar feed exhibited a 26-K noise level, while the wideband receive feed exhibited 21 K; the 5-K difference, at ambient temperature, represents 0.075 dB of dissipation loss. This unexpected condition continued during initial radar operations (December 1974 through February 1975).

In April 1975, the suspect transmit/receive switch was replaced with a spare unit in an attempt to reduce the 5-K difference in receive system noise temperatures. This was a worthwhile activity, since use of the radar in its intended mode (transmit and receive using the subreflector 1L position, as shown in Fig. 1) necessitated acceptance of significant receive system performance degradation (-10 log 26/21 or 0.9 dB) at zenith. The results were essentially as expected: the radar feed receive system noise temperature was reduced 2.5 to 23.5 K at zenith. Upon careful testing (for insertion loss), however, the original transmit/receive waveguide switch was found entirely acceptable, with 0.010 dB of dissipative loss (the value of the replacement switch). It is concluded that the noise temperature reduction of 2.5 K (about 0.04 dB) is due to the careful cleaning of the radar feed accomplished at this time. Presumably, some contamination was responsible for the added insertion loss. This hypothesis is not completely acceptable, however, since such a high loss (nearly 1% absolute) would lead to extremely hot particulate temperatures within the waveguide, with resultant breakdown failures. In general, high reflections are ruled out as the cause for the anomalous behavior since noise temperature is a sensitive detector of dissipation, not reflection loss.

Table 1 is a collection of available XKR feedcone data as of June 1975. The later value of total operating noise temperature for the radar feed at zenith is given (23.5 K). The overall system efficiencies are, however, unchanged in Table 1. With consideration for the data scatter (Fig. 12) and the estimated absolute accuracies, the small difference (0.04 dB or 0.5% efficiency at approximately 50% efficiency) goes unnoticed in the gain term. As seen in Table 1, the K-band system has not been fully checked out.

VI. Conclusions

The 400-kW X-band radar transmit feed and separate receive feed systems in the XKR feedcone system have been successfully completed in time for the initial requirements of the radar program. The major consideration in system and component design was the method used to achieve reliable switchable polarization between transmit and receive functions. The selected approach of a cylindrical waveguide rotary joint polarization switch was entirely successful despite (1) the relatively unknown electric field conditions within the rotary joint choke regions and (2) the relatively unknown harmonic output content of the unfiltered klystron (and resultant complex fields with increased breakdown risk). A totally reliable backup approach of a fixed-polarized feed, which was to have depended on subreflector switching to provide the necessary reversed transmit/receive polarizations, was built and tested but not used. Except for an initial horn aperture window failure, no erratic behavior has been experienced with the feed. It is unlikely that any arcs have occurred in the total feed assembly.

Despite the success of the key feed component (polarization switch), the actual operating mode of the radar at this time makes use of the subreflector switching mode. This is due to the operating noise levels of the two available receive paths which, at zenith, are 23.5 K (26.5 K during December 1974 to March 1975) for the radar receive and 21.5 K for the wideband receive systems. This difference in signal-to-noise performance (formerly 0.9 dB, now 0.4 dB) remains sufficiently great for experimenters to favor the lower-noise system. The difference is due to two additional components in the radar receive path (compared with the wideband receive path); a transmit/receive waveguide switch and an approximately 500-mm WR125 waveguide. The insertion loss of the additional components (0.01 dB for the switch and 0.03 dB for the waveguide) exactly account for 2.5 K of additional noise when looking out the radar receive path (see block diagram, Fig. 2). Future work towards eliminating this aspect of the system design would be useful.

Although the high-power radar feed system has been successful to date, rather minimal operating time has accumulated. The equipment must be recognized for what it is: quite new in R&D terms and extremely highly stressed in power-level terms. Lack of attention to proper servicing (nicked or broken waveguide flange, admittance of debris into the waveguide or horn, nitrogen pressurization failure) will provide a virtual guarantee of erratic (and possibly dangerous) operations. It is advised that above average attention be devoted to the care of this equipment.

Finally, mention of possible future work is made. The use of a recently developed dual-hybrid-mode feedhorn (Ref. 7) was considered at the outset of the radar project. The R&D nature of the improved feedhorn at the time and the total lack of use experience weighed against its

adoption for the time-constrained radar development. An important element of any future radar upgrade should be the new horn, which provides 0.3 dB one-way (0.6 dB radar system) advantage. The basic XKR feedcone roof structure is built to accommodate the above option. It should be recognized, however, that major internal waveguide rearrangements would be needed, both to the radar itself and the wideband radio science and DSN development front end equipments. Such a future upgrade could be doubly advantageous if combined with a decision to relocate the existing X-band maser or add an unshared X-band maser fully dedicated to the radar.

References

1. Reid, M. S., Clauss, R. C., et al., "Low-Noise Microwave Receiving Systems in a Worldwide Network of Large Antennas," *Proc. IEEE,* Vol. 61, No. 9, September, 1973, pp. 1330–1335.
2. Batelaan, P. D., and Reid, M. S., "Improved RF Calibration Techniques: MXK Cone (Mod 0) Waveguide and Noise Temperature Calibrations," in *The Deep Space Network,* Space Programs Summary 37-62, Vol. II, pp. 78–81, Jet Propulsion Laboratory, Pasadena, Calif., March 31, 1970.
3. Freiley, A. J., "Radio Frequency Performance of DSS-14 64-m Antenna at 3.56- and 1.96-cm Wavelengths," in *The Deep Space Network Progress Report,* Technical Report 32-1526, Vol. XIX, pp. 110–115, Jet Propulsion Laboratory, Pasadena, Calif., February 15, 1974.
4. Batelaan, P. D., "Waveguide Voltage Reflection Calibrations of the MXK Cone (Mod 1)," in *The Deep Space Network Progress Report,* Technical Report 32-1526, Vol. VI, pp. 123–129, Jet Propulsion Laboratory, Pasadena, Calif., December 15, 1971.
5. Buchanan, H. R., "X-Band Uplink Microwave Components," in *The Deep Space Network Progress Report,* Technical Report 32-1526, Vol. XII, pp. 22-25, Jet Propulsion Laboratory, Pasadena, Calif., December 15, 1972.
6. Brunstein, S. A., "A New Wideband Feed Horn with Equal E- and H-Plane Beamwidths and Suppressed Sidelobes," in *The Deep Space Network,* Space Programs Summary 37-58, Vol. II, pp. 61–64, Jet Propulsion Laboratory, Pasadena, Calif., July 31, 1969.
7. Thomas, R. F., and Bathker, D. A., "A Dual Hybrid Mode Feedhorn for DSN Antenna Performance Enhancement," in *The Deep Space Network Progress Report 42-22,* pp. 101–108, Jet Propulsion Laboratory, Pasadena, Calif., August 15, 1974.

Table 1. XKR feedcone characteristics

XKR feedcone system	Overall system efficiency, gain tolerance, and T_{op} at 8495 MHz					Primary frequency range, MHz	Usable frequency range, MHz
	η, % 20-deg EL	η, % 45-deg EL	η, % 70-deg EL[a]	Estimated system gain tolerance (3σ) absolute, dB	Total operating system noise temperature at zenith (T_{op}), K		
Radar transmit feed[b]	40	43	42	+0.3 −0.8	N/A[c]	8495 ±10	8400–8700
Wideband receive feed[d]	43	46	45	+0.2 −0.7	21.0	7800–7900 8400–8500	7750–8800
Radar receive feed[d] (Use of TX horn for both functions)	42	45	44	+0.2 −0.7	23.5	8495 ±10	8400–8700
K-band receive feed	N/A	N/A	N/A	N/A	N/A	15,000–16,000	14,500–16,500

[a]Values determined from curve fit through data but extended beyond the range of measured data.

[b]From power combiner output, including losses; estimated efficiencies.

[c]N/A = not available.

[d]Referenced to the TWM input; measured efficiencies.

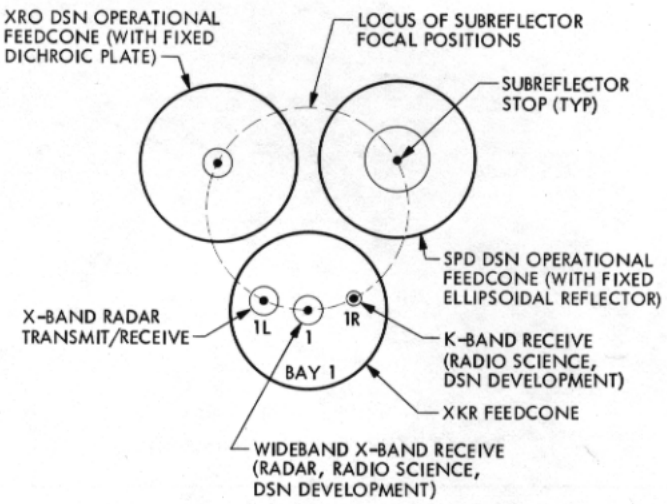

Fig. 1. Face view of DSS 14 tricone

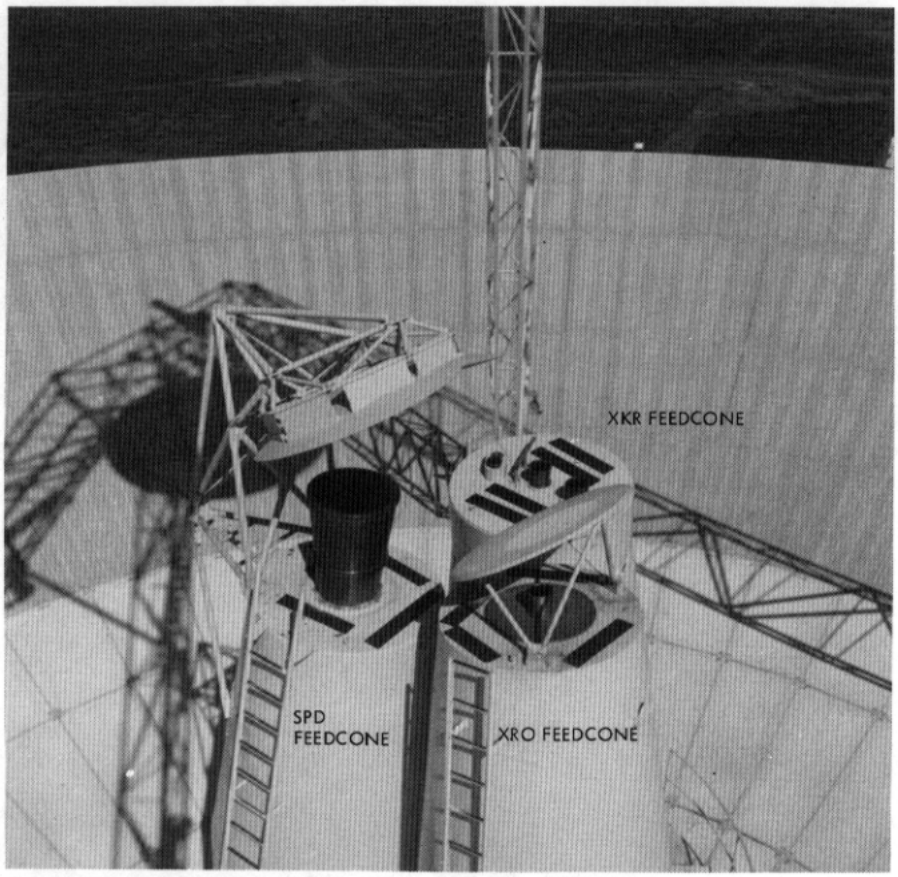

Fig. 2. Tricone feed system at DSS 14

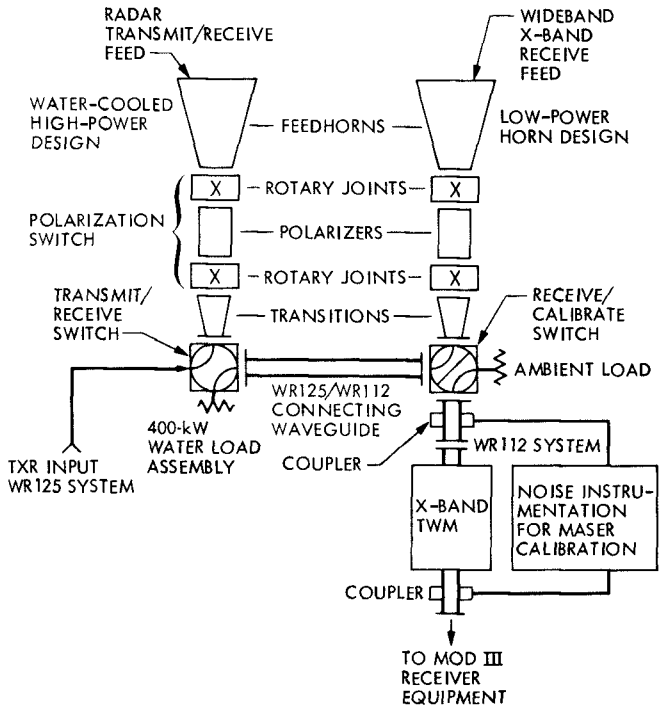

Fig. 3. XKR feed cone, X-band block diagram

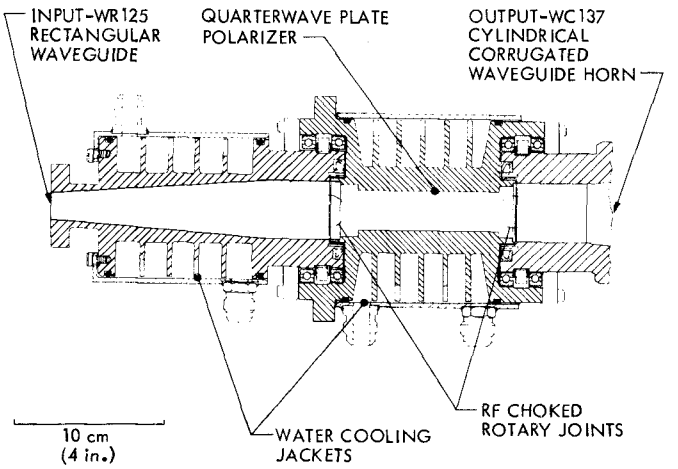

Fig. 4. Radar feed assembly

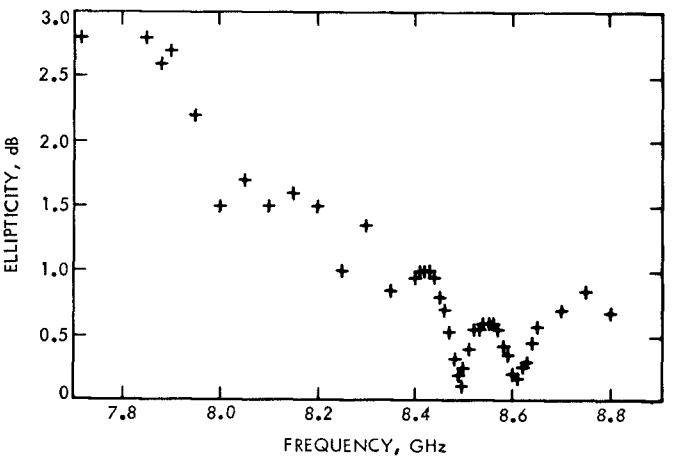

Fig. 5. Radar feed system ellipticity

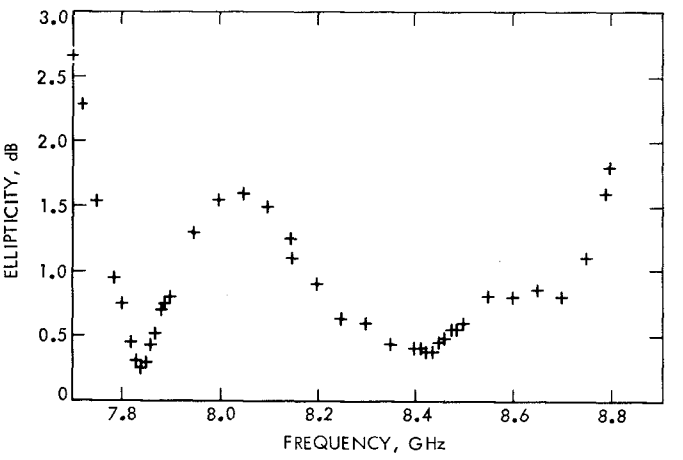

Fig. 6. Wideband receive feed sytem ellipticity

Fig. 7. Radar feed assembly power tests

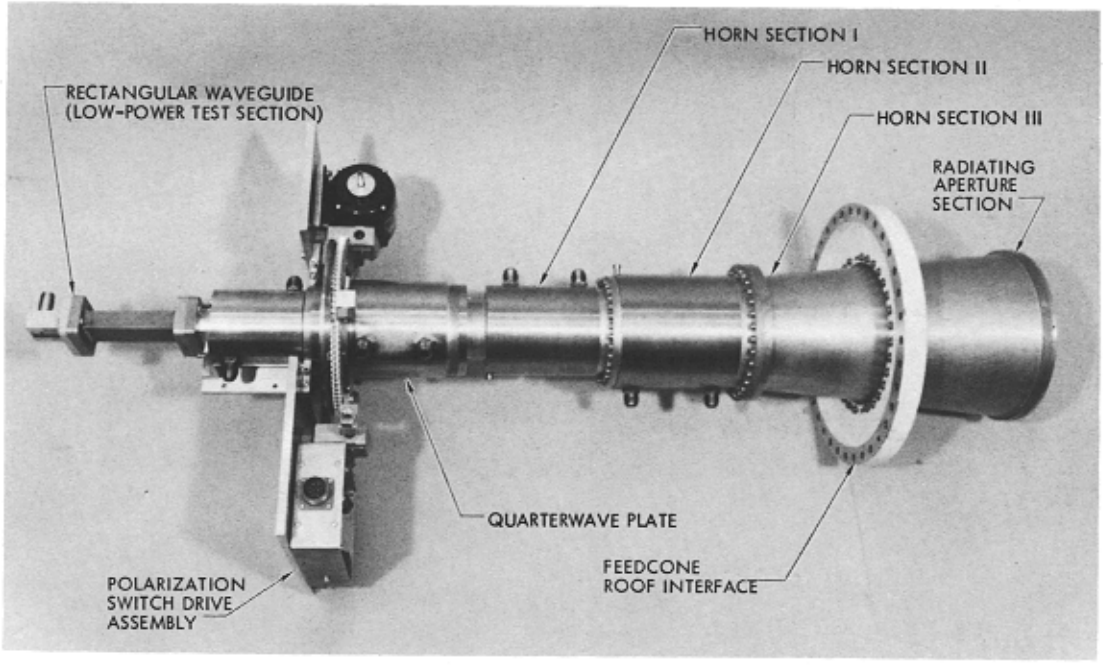

Fig. 8. X-band radar feed assembly

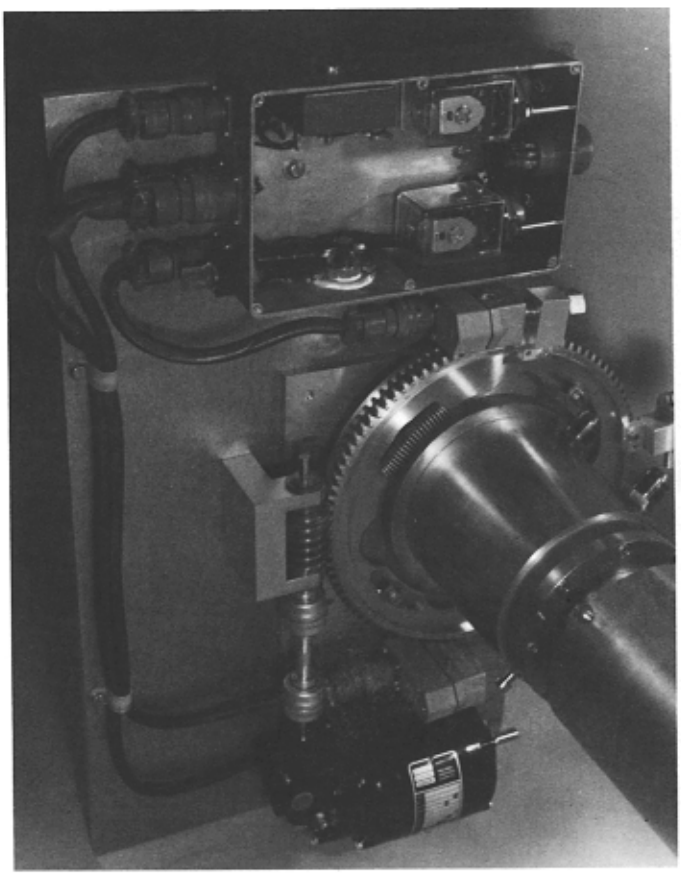

Fig. 9. Polarization switch drive

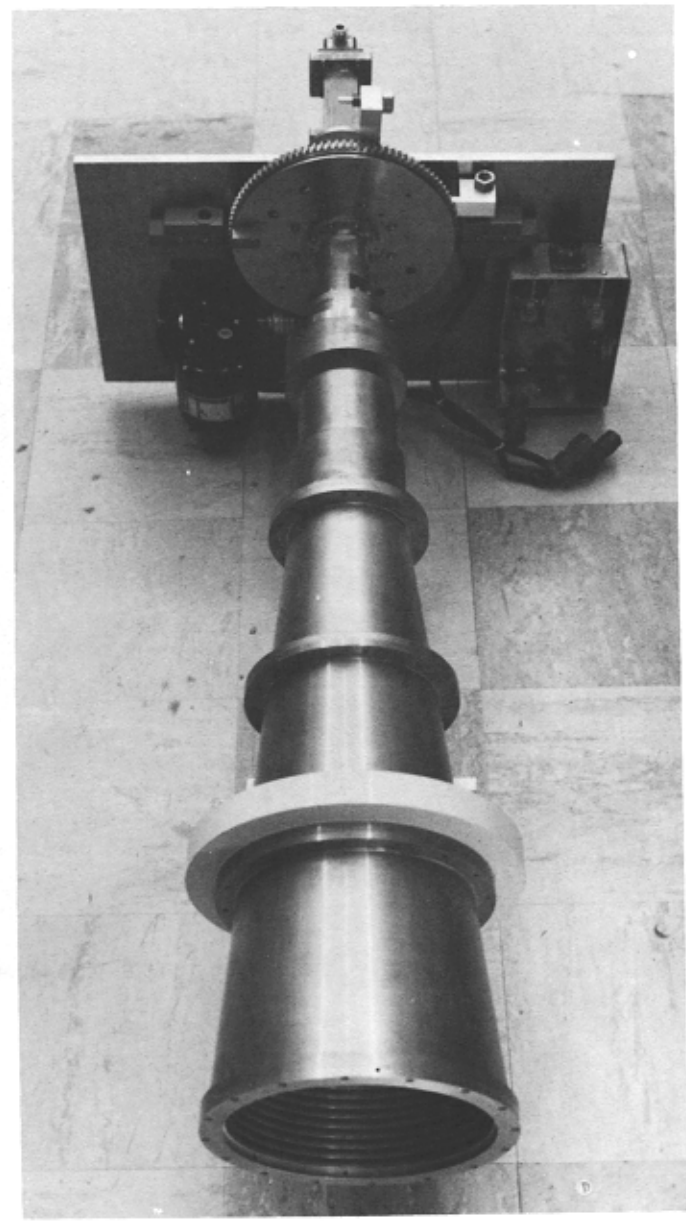

Fig. 10. Wideband receive feed

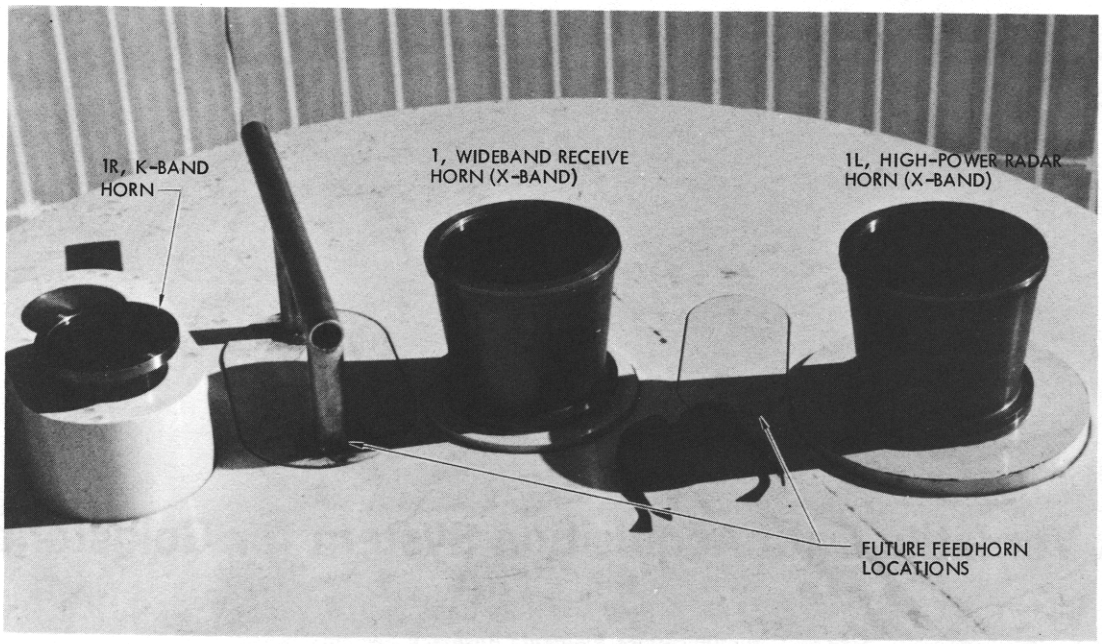

Fig. 11. XKR feedcone roof

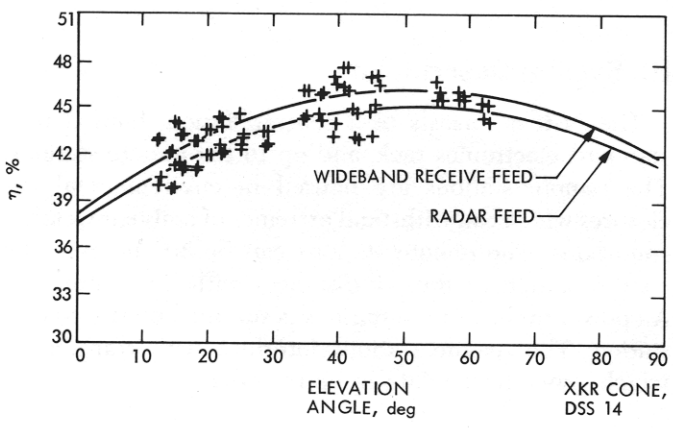

Fig. 12. Overall system efficiency vs. elevation angle

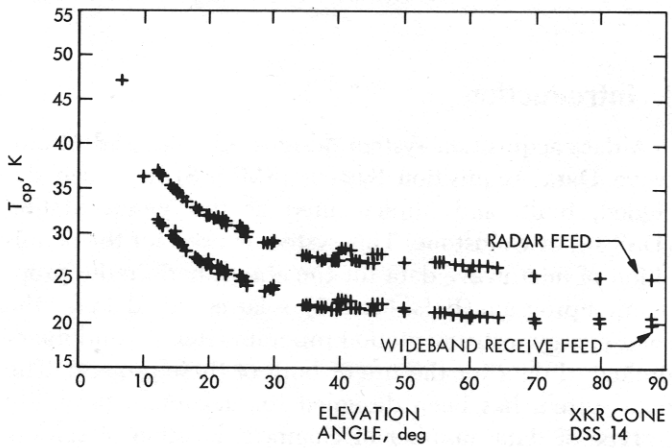

Fig. 13. Operating system noise temperature vs. elevation angle